Talanta 127 (2014) 9–17

Contents lists available at ScienceDirect

Talanta

journal homepage: www.elsevier.com/locate/talanta

Cholinesterase sensor based on glassy carbon electrode modified with Ag nanoparticles decorated with macrocyclic ligands

Gennady A. Evtugyn [a,*], Rezeda V. Shamagsumova [a], Pavel V. Padnya [b], Ivan I. Stoikov [b], Igor S. Antipin [b]

[a] Analytical Chemistry Department of Kazan Federal University, 18 Kremlevskaya Street, Kazan 420008, Russian Federation
[b] Organic Chemistry Department of Kazan Federal University, 18 Kremlevskaya Street, Kazan, 420008, Russian Federation

ARTICLE INFO

Article history:
Received 27 January 2014
Received in revised form
14 March 2014
Accepted 19 March 2014
Available online 3 April 2014

Keywords:
Acetylcholinesterase
Biosensor
Ag nanoparticles
Inhibition measurement
Pesticide detection

ABSTRACT

New acetylcholinesterase (AChE) sensor based on Ag nanoparticles decorated with macrocyclic ligand has been developed and successfully used for highly sensitive detection of organophosphate and carbamate pesticides. AChE was immobilized by carbodiimide binding on carbon black (CB) layer deposited on a glassy carbon electrode. The addition of Ag nanoparticles decreased the working potential of the biosensor from 350 to 50 mV. The AChE sensor made it possible to detect 0.4 nM–0.2 μM of malaoxon, 0.2 nM–0.2 μM of paraoxon, 0.2 nM–2.0 μM of carbofuran and 10 nM–0.20 μM of aldicarb (limits of detection 0.1, 0.05, 0.1 and 10 nM, respectively) with 10 min incubation. The AChE sensor was tested for the detection of residual amounts of pesticides in spiked samples of peanut and grape juice. The protecting effect of new macrocyclic compounds bearing quaternary ammonia fragments was shown on the example of malaoxon inhibition.

1. Introduction

The development of instrumental tools for sensitive detection of enzyme inhibitors is of substantial interest in the environmental, food and agricultural areas [1]. Among others, organophosphate and carbamate pesticides exert irreversible inhibition of acetylcholinesterase (AChE). The pesticides or their primary metabolites form a covalent bond between the hydroxyl group of serine residue of the enzyme active site and esteric fragment of an inhibitor molecule [2,3]. The product of the reaction, i.e. phosphorylated or carbamoylated AChE does not react with a substrate. This results in a decrease of the enzyme activity quantified by appropriate transducer. The carbamoylated AChE is spontaneously re-activated in aqueous media so that maximal inhibition levels can be beyond 100%. The product of organophosphate inhibition is commonly stable and the enzyme activity decreases down to zero with an increase of the inhibitor concentration and/or incubation period.

The necessity of the detection of organophosphates and carbamates is related to the AChE biological function. This enzyme is widely present in warm-blooded living beings and is responsible for the nerve impulse transduction by hydrolysis of a natural neurotransmitter, acetylcholine.

$$\underset{\text{Acetylcholine}}{(CH_3)_3N^+CH_2CH_2O\overset{\displaystyle O}{\overset{\|}{C}}CH_3} + H_2O \xrightarrow{\text{AChE}} \underset{\text{Choline}}{(CH_3)_3N^+CH_2CH_2SH} + CH_3COOH \quad (1)$$

The inhibition of AChE in living beings increases the concentration of acetylcholine followed by abdominal cramps, muscular tremor, hypotension, breathing difficulty, slow heartbeat and death [4,5].

The residual amounts of anticholinesterase pesticides in soils, vegetables, biological tissues and food are commonly determined by gas chromatography with mass spectrometry [6,7] and flame photometry detection [7] and liquid chromatography with fluorescence/UV [8], diode-array [9] and mass spectrometry [10] detection. For sample pre-concentration, liquid–liquid [10] and solid-phase extraction techniques are often used [11]. The chromatographic detection of pesticides is summarized in recent review [12]. From other techniques, immunoassay in ELISA [13], fluorescent polarization [14] and lateral flow format [15] can be mentioned.

AChE biosensors are compact devices developed for the fast and sensitive detection of pesticides, preferably in field conditions.

* Corresponding author.
E-mail addresses: gennady.evtugyn@kpfu.ru, gevtugyn@gmail.com (G.A. Evtugyn).

http://dx.doi.org/10.1016/j.talanta.2014.03.048
0039-9140/

They do not compete with conventional instrumental tools but can be used for preliminary estimation of potential hazard related to anticholinesterase species. For electrochemical detection, the following strategies have been realized for the AChE inhibition quantification in past two decades: (i) the use of choline oxidase for subsequent oxidation of choline released in reaction (1) and detection of hydrogen peroxide produced [16]; (ii) the potentiometric determination of the amounts of acetic acid released [17]; and (iii) the use of artificial substrate, acetylthiocholine (ATCh), which produces electrochemically active thiocholine oxidized on the electrode (2).

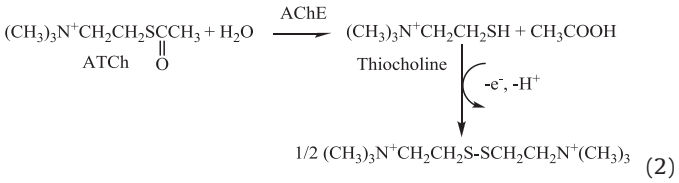

(2)

The latter approach showed some advantages, i.e. simpler design of a biosensor, higher sensitivity and accuracy of the signal measurement and extended lifetime of the biosensor. Direct oxidation of thiocholine on metal and glassy carbon electrodes can be performed with rather high over voltage at 450–680 mV. The oxidation is complicated with partial poisoning of the electrode and accumulation of chemisorbed by-products affecting the reproducibility of the current recorded. Various mediators and their combinations have been proposed for AChE sensors, i.e. carbon nanotubes [18–20], ferricyanide [21], Prussian Blue [22–24], tetracyanoquinodimethane [25], and Co phthalocyanine [26–28].

In addition to them, Au nanoparticles have found application for both signal transduction and enzyme immobilization via Au–S bonds [19,23,29,30]. Silver is an alternative for gold in the assembly of biosensors. Being less hydrophobic and more reactive, Ag nanoparticles can be easily obtained in situ on the transducer surface in mild conditions compatible with those of enzyme immobilization. Meanwhile, Ag nanoparticles require additional stabilization and protection from undesired chemisorption of the reactants.

Recently, two Ag electrodes have been successfully used for the detection of thiocholine as a product of enzymatic reaction. A flow injection system with a silver electrode on-line was described for the amperometric detection of thiocholine liberated up-front in a flow-through detector [31]. AChE was immobilized on a golden support. The response was generated by oxidation of silver in the presence of thiocholine at about 80 mV. The comparison of thiocholine oxidation on Ag, Pt, glassy carbon and Au showed the lowest potential of 0.08 V on silver electrode used then for paraoxon detection [32].

In this work we have described a simple and reliable protocol for the synthesis of Ag nanoparticles in the reaction of thiacalix[4]arene bearing catechol fragments in the substituents at the lower rim. The macrocycle applied as a reducing agent shields the surface of nanoparticles from aggregation and dissolution and also provides reversible and fast electron exchange on the electrode interface. The electrodes modified with Ag nanoparticles decorated with macrocyclic ligands were successfully applied for dopamine detection [33] and as a transducer in the aptasensor for ochratoxin A determination [34]. In this work, we recommend the AChE sensor with glassy carbon electrode modified with Ag nanoparticles for the detection of anticholinesterase pesticides and protective agents testing.

2. Experimental

2.1. Reagents

AChE from electric eel (687 U/mg prot.), *N*-(3-dimethylaminopropyl)-*N*′-ethylcarbodiimide chloride (EDC), 2-(*N*-morpholino) ethanesulfonic acid (MES), *N*-hydroxysuccinimide (NHS), 2-pyridine aldoxime (2-PAM), ATCh chloride were purchased from Sigma (St Louis, MO). Malaoxon (Pestanal, stock solution 1 mg/mL in ethanol), malathion (Pestanal, 97.2% solid), paraoxon (96% solid), aldicarb (Pestanal, 99.9% solid) and carbofuran (Pestanal, 99.9% solid) were purchased from Fluka (Germany). Carbon black (CB, N220) of industrial standard grade was obtained from Cabot Corporation (Ravenna, Italy). All other reagents were of analytical grade.

5,11,17,23-Tetra-*tert*-butyl-25,26,27,28-tetrakis-[1-(2′-hydroxyethyl)-*N*-(3″,4″-dihydroxyphenyl)amidocarbonyl)-methoxy)-2,8,14,20-tetrathiacalix[4]arene in *1,3-alternate* conformation (**TC-0**) was synthesized as described elsewhere [33]. For the synthesis of Ag nanoparticles, 0.01 M stock solution of the thiacalix[4]arene in acetone was prepared and then diluted with 50% (v/v) aqueous acetone prior to use.

The following thiacalix[4]arenes bearing quaternary ammonia groups at the substituents at the lower rim have been tested (Fig. 1): 5,11,17,23-Tetra-*tert*-butyl-25,26,27,28-tetrakis-[(*N*-(30,30,30-trimethylammoniumpropyl)carbamoylmethoxy)]-2,8,14,20-thiacalix[4]arene tetranitrate (**TC-1**). 5,11,17,23-tetra-tert-butyl-25,26,27,28-tetrakis-[(*N*-phthalimideammoniumpropyl) carbamoylmethoxy]-2,8,14,20-thiacalix[4]arene tetranitrate (**TC-2**), 5,11,17,23-tetra-tert-butyl-25,26,27,28-tetra-[(*N*-(3′,3′-dimethyl-3′-ethylammoniumpropyl) carbamoylmethoxy]-2,8,14 20-thiacalix[4]arene tetranitrate (**TC-3**), 5,11,17,23-tetra-tert-butyl-25,26,27,28-tetrakis-[(*N*-(30,30-dimethyl-30-benzylammoniumpropyl)carbamoylmethoxy)]-2,8,14,20-thiacalix[4]arene tetranitrate (**TC-4**). All the thiacalix[4]arenes were synthesized at the Organic Chemistry Department of Kazan Federal University in accordance with [35] as iodide salts. Their structure and purity were confirmed by NMR ^{1}H and ^{13}C, IR-spectroscopy, MALDI-TOF and elemental analysis. Prior to use, all the thiacalix[4]arenes were treated with $AgNO_3$ to get nitrate salt forms. The anion exchange was monitored by Dionex ICS 5000 (Thermo Fischer Scientific Inc., USA).

Electrochemical measurements were performed in PBS (0.05 M disodium phosphate + 0.1 M NaCl) adjusted to pH 7.8. For electrode washing, 1.0 M NaCl solution containing 0.05 M phosphate buffer and 0.1 M ethanolamine was used. The substrate and inhibitor solutions were prepared directly prior to their use in measurements by aliquot dilution of stock solutions by Millipore Q® water. The ATCh stock solution was stored at 4 °C for not more than one week.

2.2. Apparatus

Electrochemical measurements were performed with AUTOLAB PGSTAT 302N potentiostat with FRA module for electrochemical impedance (EIS) measurements (Metrohm Autolab B.V., The Netherlands). Three-electrode cell with glassy carbon electrode (working area 1.67 mm^2), Pt auxiliary electrode and double junction Ag/AgCl reference electrode (AUTOLAB Cat. no. 6.0726.100) were used in all the electrochemical measurements.

EIS spectra were recorded using NOVA software (Metrohm Autolab B.V., The Netherlands) in the presence of 0.01 M $K_3[Fe(CN)_6]$ and 0.01 M $K_4[Fe(CN)_6]$. The amplitude of the applied sine potential was 5 mV. The direct current potential was calculated as half-sum of the peak potentials of the redox couple $[Fe(CN)_6]^{3-/4-}$. The EIS spectra were recorded within the frequency from 100 kHz to 0.04 Hz with a sampling rate of 12 points per decade.

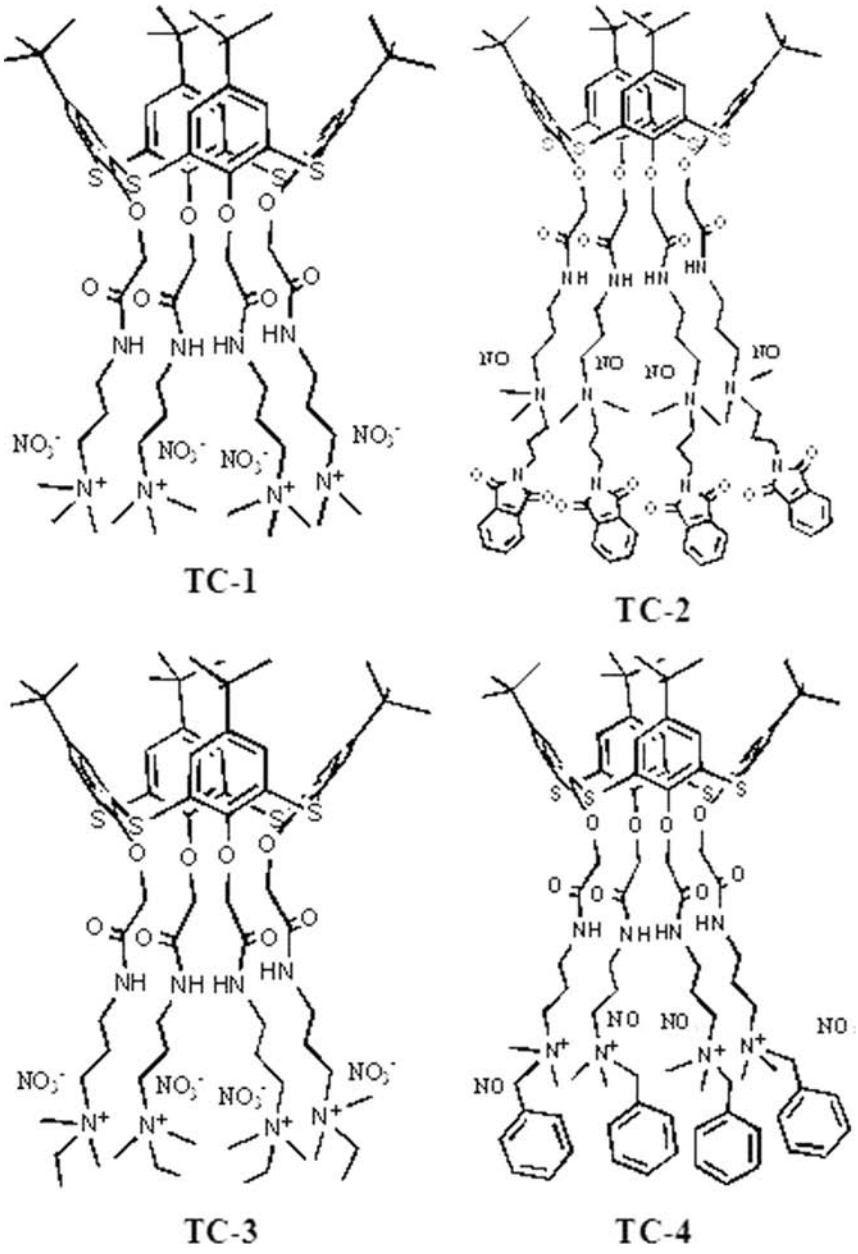

Fig. 1. Substituted thiacalix[4]arenes tested as protecting agents for irreversible AChE inhibition.

The calculations of capacitance and resistance from EIS spectra were made using fitting procedure corresponding to the equivalent circuits shown as follows:

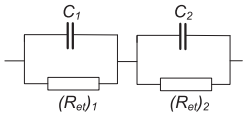

(3)

where R_{et} is an electron transfer resistance and C the capacitance of the electrode surface. The indices 1 and 2 correspond to the inner (electrode–modifier) and outer (modifier–solution) interfaces. The dimensionless "roughness" index n was higher than 0.88 in all the experiments, so that pure capacitance C can be used instead of the constant phase element (CPE) expressing non-ideal capacitive response of the interface.

2.3. Glassy carbon electrode modification

For the synthesis of Ag nanoparticles, 250 μL of 0.1 mM **TC-0** solution in acetone was mixed with 20 μL of 0.01 M aqueous $AgNO_3$ solution and 2.5 μL of 0.01 M triethylamine in acetone. The mixture was left in dark for 30 min. Reaction (4) results in the formation of silver nanoparticles. In accordance with previous TEM investigation [33,34], 15–20 nm Ag nanoparticles are uniformly distributed in organic matrix.

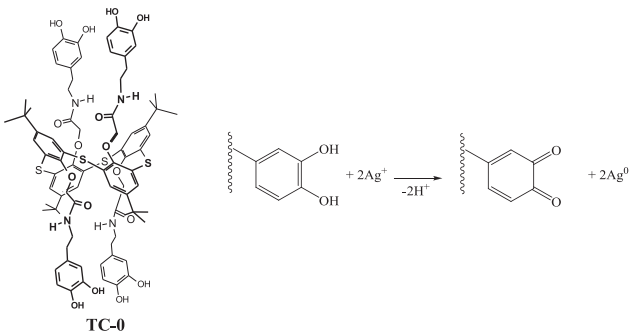

(4)

Prior to modification, glassy carbon electrode was mechanically polished and cleaned with 1.0 M sulfuric acid, NaOH and acetone. After that, the electrode was dried and fixed upside down. 2 μL of CB suspension prepared by 30 min sonication of 1 mg/mL dispersion in dimethylformamide was dispersed on the working area and dried at 70 °C for 20 min. After that, 2 μL of Ag nanoparticles dispersion was placed on the CB layer and the electrode was dried at ambient temperature for 30 min.

2.4. AChE immobilization

The electrode modified with CB and Ag nanoparticles was fixed upside down and treated with 5 μL of 15 mM EDC and 5 μL 8.7 mM NHS in 0.05 M MES buffer (pH=5.5). After that, the electrode was covered with a plastic tube for 30 min to avoid drying and washed twice with Millipore water and finally with PBS (pH=7.8). Then 2 μL of the AChE solution with specific activity of 1.5–25 U/mL was poured onto the electrode surface. The electrode was dried and washed twice with Millipore water and BPS buffer solution to remove unbounded enzyme molecules from the surface. The AChE sensors were stored in 0.05 M PBS buffer between measurements. In some experiments, the ATCh hydrolysis was performed by addition of 1 U/mL of AChE to the 0.1 mM ATCh solution followed by 15 min incubation at ambient temperature.

2.5. ATCh and pesticide determination

The operability of the AChE sensor was checked by cyclic voltammetry by recording the reversible peak in the area of 120–170 mV after the injection of 0.1 mM ATCh solution. The measurements of signals toward ATCh and anticholinesterase pesticides were performed in chronoamperometric regime at constant potential of 150 mV by consecutive injection of analyte solution and recording current changes. Between measurements of the substrate signal and inhibitor addition, the AChE sensor was washed with PBS buffer for 5 min to remove excessive amounts of the substrate from the surface layer.

The irreversible inhibition was quantified by inhibition degree calculated as relative decay the oxidation current recorded after 10 min incubation of the AChE sensor in the pesticide solution. In some experiments, the inhibited AChE was re-activated by 10 min treatment with 0.1 mM 2-PAM solution. The protecting effect of thiacalix[4]arenes **TC-1**–**TC-4** was estimated in a similar manner by incubation of the AChE sensor in the mixture of thiacalix[4]arene and pesticide.

Peanut and grape juice were purchased from local suppliers; HPLC analysis did not show the residuals of anticholinesterase pesticides which might affect the results of inhibition detection. Spiked samples of peanut were prepared by carefully grinding the peanuts followed by the addition of pesticide solution in acetone. After 24 h incubation the solvent was evaporated and the grinded peanut was applied for anticholinesterase effect testing. The grape juice was mixed with an aliquot of pesticide solution in acetone or acetonitrile with the final portion of organic solvent less than 1 vol %. The spiked sample of grape juice was then used for inhibition measurement without any other pretreatment. Malathion was oxidized to malaoxon by treatment with bromine water followed by removal of excessive amount of oxidant with formic acid and pH adjustment.

All the experiments were performed in six repetitions with a set of the AChE sensors prepared with the same reagent solutions.

3. Results and discussion

3.1. Voltammetric characterization of the modifying layer

The preliminary results on the electrochemical behavior of **TC-0** in aqueous acetone solution and on the electrode surface as well as TEM images confirming the formation of silver nanoparticles were presented before [33,34]. The deposition of CB on the glassy carbon electrode does not lead to the electrochemical activity in the potential region typical for thiocholine or silver oxidation. The addition of Ag nanoparticles results in remarkable changes in cyclic voltammograms which depend on the conditions of Ag^+ reduction. If the amount of thiacalix[4]arene **TC-0** used as reducing agent is below than that required for full reduction of Ag^+ ions (molar ratio **TC-0**: Ag^+ = 1:8 for simultaneous oxidation of four catechol fragments of a thiacalix[4]arene molecule, see scheme (2)), a sharp peak at about 30 mV is observed in the first scans of the potential (Fig. 2). It can be related to anodic dissolution of naked Ag nanoparticles on the electrode surface. The position of the peak is not shifted with the AChE immobilization whereas the peak current decreases by about 60% due to shielding metal particles by protein layer. The peak current progressively decreases with the number of potential cycles. Instability of the Ag peak does not allow its application for substrate/inhibitor determination.

In addition to the peak referred to free Ag particles, a broaden peak at 300–350 mV was observed on direct scan. Contrary to oxidation of naked Ag nanoparticles its position was found to be quite stable in multiple cycling. The peak current progressively increased with the aliquot of Ag nanoparticles suspension placed on the electrode. Although the height of the peak was by 25–30% lower than that at 30 mV, the peak area was 3–4 times higher. The ratio of the peak square recorded at 30 and 350 mV changed in accordance with relative excess of Ag^+ ions over stoichiometric ratio in the mixture used for suspension preparation. This made it

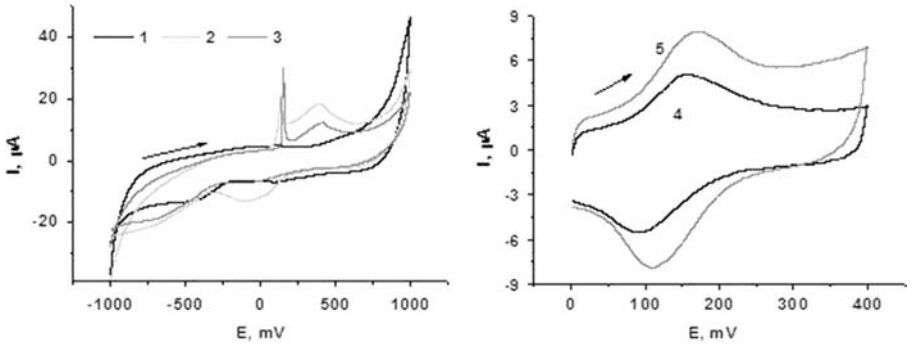

Fig. 2. Cyclic voltammograms recorded on glassy carbon electrode modified with CB (1), CB and Ag nanoparticles (2, 4) prior to (1, 2) and after immobilization of AChE (3). Molar ratio of **TC-0** and Ag^+ 1:10 (1–3) and 1:8 (4, 5). The effect of 0.1 mM of thiocholine obtained by enzymatic hydrolysis of ATCh in solution (5). Measurements in PBS, pH=7.8, scan rate 50 mV/s.

possible to conclude that the peak at 350 mV is related to Ag nanoparticles decorated with **TC-0** molecules.

This explanation coincides well with the changes of voltammograms obtained for the stoichiometric ratio of **TC-0** and Ag^+ ions or insignificant excess of **TC-0** in the reaction mixture. The anodic peak at 30 mV disappeared whereas the peak at 350 mV becomes reversible and increases in the presence of thiocholine obtained by enzymatic hydrolysis of ATCh in solution (Fig. 2b). The stability and reversibility of the peak at 350 mV is due to involvement of catechol fragments of **TC-0** in the electron transduction as well as coordination of Ag^+ within the core shell on the anodic branch of the cycle. This prevents the ions from leaching and provides their reversible cathodic deposition on the electrode. The electrochemical characteristics of **TC-0** taken alone and together with Ag nanoparticles in suspension and on the surface of electrode were described in [33]. As shown above, Ag nanoparticles accelerate the electron transfer and promote the involvement of macrocyclic ligands in the reversible electron exchange on the electrode interface. It should be mentioned that the addition of thiocholine obtained by enzymatic hydrolysis of ATCh in homogeneous conditions equally increased the cathodic and anodic peaks at 300–350 mV. This made it possible to conclude that the Ag nanoparticles provide chemisorption accumulation of thiocholine followed by its oxidation via macrocyclic surrounding. In alternative mechanism (direct electrocatalysis), an increase of anodic peak followed by decreasing cathodic peak and shift of the formal potential to less positive values would be observed.

3.2. EIS measurements

EIS is a powerful tool for the investigation of electron transfer on the electrode interface. The comparison of the electron transfer resistance and the capacity of the surface layer makes it possible to specify the role and significance of modifier on the biosensor performance. The equivalent circuit (3) with two parts reflecting inner (electrode–modifier) and outer (modifier–solution) interfaces of the biosensor was used for the calculation of the EIS parameters. Measurements were performed in the presence of ferricyanide ions. Their formal redox potential insignificantly varied between 210 and 230 mV with deposition of various layers onto glassy carbon surface. Although the formal potential of $[Fe(CN)_6]^{3-/4-}$ was quite similar to that of Ag–**TC-0** layer, no evidence of electron exchange within surface layer was observed. The peaks of ferricyanide ions on voltammogram remained symmetrical with the peak potential difference of about 110 mV indicating quasi-reversible character of electrode reaction. The EIS characteristics of electrodes modified with CB, Ag nanoparticles and AChE are presented in Table 1.

The addition of CB increases the capacity of the surface layer due to own charge of carboxylic groups and increased surface area. The effect is pronounced on the inner interface where the modifier directly contacted with glassy carbon. Contrary to that, changes in the capacity are much higher on the outer interface due to electrostatic repulsion of negatively charged ferricyanide ions and carboxylate groups of the surface layer. The immobilization of AChE partially suppresses the influence of CB on the EIS parameters due to involvement of carboxylic groups in the carbodiimide binding of enzyme and due to formation of a protein layer on the surface of conducting material. The presence of the Ag nanoparticles positively affects the conditions of the electron transfer on the electrode interface whereas its influence on outer interface is insignificant taking into account rather high variation of the parameters. This coincides well with the suggestion about predominant effect of electrostatic interactions of the electron transfer parameters because both the Ag nanoparticles and their aggregates with **TC-0** do not carry remarkable charge comparable with that of carboxylic groups ionized in the measurement conditions (pH = 7.8).

Table 1
The EIS characteristics of glassy carbon electrode modified with CB, Ag nanoparticles and AChE. Measurements in the presence of 0.01 M $K_3[Fe(CN)_6]$ and 0.01 M $K_4Fe(CN)_6$, PBS, pH = 7.8 (n = 6).

Modifier	Inner interface		Outer interface	
	$(R_{et})_1$ (kΩ)	C_1 (μF)	$(R_{et})_2$ (kΩ)	C_2 (μF)
–	1.76 ± 0.35	4.9 ± 2.3		
CB	0.31 ± 0.05	21.7 ± 7.3	1.26 ± 0.15	1055 ± 330
CB–Ag	0.47 ± 0.11	7.2 ± 2.6	1.35 ± 0.06	460 ± 100
CB–AChE	0.35 ± 0.07	4.8 ± 1.3	0.98 ± 0.08	525 ± 115
CB–Ag–AChE	0.90 ± 0.18	22.0 ± 5.5	1.81 ± 0.16	350 ± 110

3.3. Chronoamperometric measurements

Cyclic voltammetry experiments have shown that the current of the peak at 350 mV regularly changes with the thiocholine concentration. This offers opportunities for the detection of ATCh and AChE inhibition after the enzyme immobilization. Meanwhile the regime of potential cycling is less convenient for biosensor format so that the following experiments were performed in chronoamperometric regime at a constant potential of the AChE sensor. As was shown, the oxidation current increased with the ATCh injection in the range from 50 to 300 mV with maximal response at 50 and 150 mV (Fig. 3). The time corresponding to 95% of the shift of the current did not exceed 20 s.

The characteristics of ATCh determination corresponding to the initial part of calibration curve approximated with linear fit are presented in Table 2. One can see that the maximal sensitivity and minimal LOD value (4 μM) were obtained for working potentials of 100 and 150 mV. The maximal signal corresponding to the saturation of the surface layer did not alter significantly with the working potential.

The apparent value of Michaelis constant $(K_m)_{app}$ calculated in the plots of $1/I$ against $1/c$ was found to be 0.062 ± 0.034 mM. This is comparable with the values reported for free enzyme in similar conditions (0.1 mM [36,37]). This indicates no steric limitations of the access of enzyme active site for the substrate molecules. Some other AChE sensors showed similar $(K_m)_{app}$ values: 0.67 mM (entrapment of AChE in hydrophilic polymeric films [38], 0.45 mM (metal-affinity immobilization via histidine tags [38]), and 0.22 mM (affinity immobilization via concanavalin A [36]).

Similar experiments with the AChE sensor based on the CB modified glassy carbon electrode showed that increase in current started from 300 mV, i.e. at the potential 250 mV higher than that in the presence of Ag nanoparticles. The maximal level of the current reached at the saturation of the surface layer with the substrates remained the same. This confirms the mechanism of AChE immobilization via CB carboxylic groups with no participation of Ag nanoparticles. Meanwhile the linearity region becomes narrower and the steady-state current less stable in comparison with the sensor modified with **TC-0**–Ag aggregates. The appropriate dynamic response and calibration curves obtained for various working potentials are presented in Supplementary materials (Fig. S1). Thus the use of Ag nanoparticles improves the performance of the AChE sensor in ATCh determination.

3.4. Working conditions of the signal measurement

The amounts of enzyme and pH affect the response of the AChE sensor due to changes in the substrate mass transfer in the surface layer and pH-sensitivity of the enzyme activity. The current of

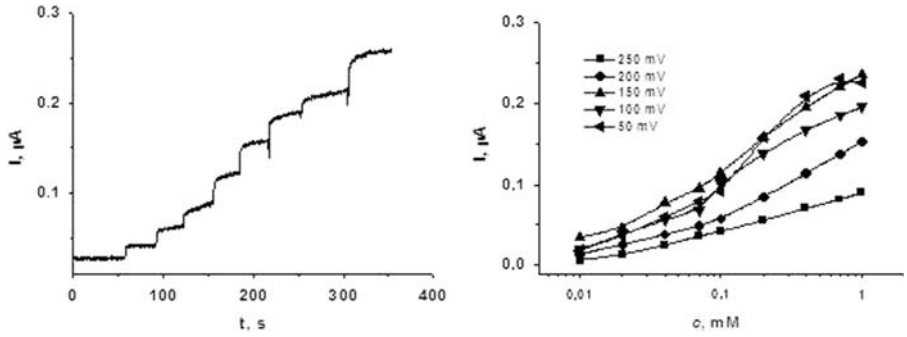

Fig. 3. Dynamic response of AChE sensor with CB, Ag nanoparticles and AChE (6.25 U/mL, aliquot 2 μL) on 20, 60 μM, 0.1, 0.2, 0.4, 1.0 and 2.0 mM ATCh at 150 mV and dependence of the signal on the working potential. Chronoamperometric regime, PBS, pH 7.8.

Table 2
The analytical characteristics of the ATCh determination with the AChE sensor based on glassy carbon electrode modified with CB, AG nanoparticles and AChE. PBS, pH 7.8.

E (mV)	I, μA= a+b × c, M				Concentration range, mM	LOD, mM
	a	*b*	R^2	*n*		
50	0.051 ± 0.010	414 ± 40	0.9429	5	0.04–0.40	0.010
100	0.027 ± 0.007	598 ± 32	0.9561	6	0.01–0.20	0.004
150	0.042 ± 0.007	626 ± 34	0.9451	6	0.01–0.20	0.004
200	0.031 ± 0.004	220 ± 12	0.9691	6	0.01–0.20	0.005
250	0.006 ± 0.003	398 ± 30	0.9391	5	0.01–0.10	0.005

thiocholine oxidation increased from 0.06 to 0.20 μA while the pH of the buffer solution was changed from 7.0 to 7.8 (ATCh 0.4 mM). The following increase of the pH value to 8.5 did not alter the signal value but increased the deviation in a series of repetitions. For this reason, inhibition measurement was performed at pH 7.8. This corresponds to the maximum of enzyme activity established in homogeneous conditions. Full calibration curves of the substrate recorded in the pH range from 7.0 to 8.0 are given in Supplementary materials (Fig. S3).

The influence of the enzyme quantities on the signal toward the substrate is shown in Fig. 4. The increase in the enzyme concentration in the aliquot results in higher sensitivity of the signal toward the substrate at low ATCh concentration and bigger saturation level of the signal. The sensitivity of inhibitor determination commonly decreases with increased surface activity of an enzyme. For this reason, the choice of enzyme loading should take into account both the signal and accuracy of its determination to improve metrological characteristics of inhibition degree calculation. For this reason, inhibition was then measured at 4.2 U/mL of AChE in the aliquot of 2 μL per electrode.

As regards other components of the surface layer, the quantities of CB are determined from the requirements of full coverage of the surface and mechanical stability of the layer obtained. The use of 2 μL of the CB suspension (1 mg/mL in dimethylformamide) was found to be optimal to extend the lifetime of the transducer. The increase of the Ag nanoparticles amounts over that used resulted in increase of the electron transfer resistance and reversibility of the peaks on voltammograms. The effect of amounts of Ag nanoparticles on electrochemical characteristics of the electron exchange has been considered in more detail in [33].

3.5. Pesticide determination

The irreversible inhibition of malaoxon, paraoxon, aldicarb and carbofuran was measured by incubation of the AChE sensor in pesticide solution in the absence of a substrate followed by measurement of decreased signal toward 0.4 mM ATCh and

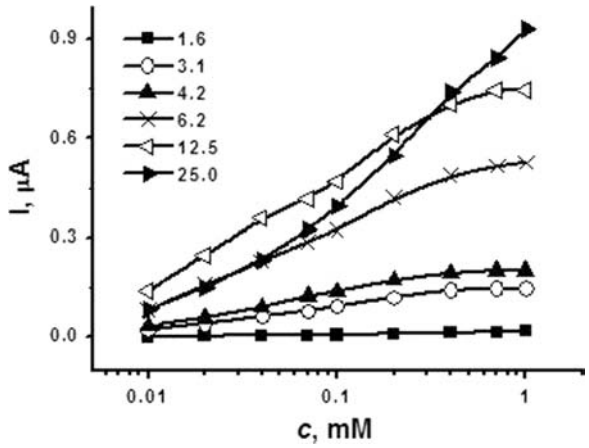

Fig. 4. Calibration plots of ATCh obtained with AChE sensors based on glassy carbon modified with CB and Ag nanoparticles and various amounts of enzyme. The specific activity of AChE in aliquot is given. The biosensors were prepared by placing 2 μL of aliquot on the electrode surface.

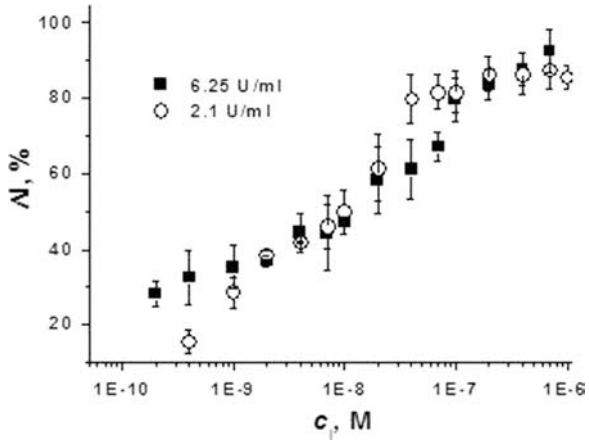

Fig. 5. Calibration plots of malaoxon obtained with AChE sensor based on glassy carbon modified with CB and Ag nanoparticles and various amounts of enzyme. Incubation 10 min, PBS, pH = 7.8.

calculation of inhibition degree. The concentration of a substrate corresponds to the saturation of the surface layer and hence maximal sensitivity of inhibition measurement.

A typical calibration curve of malaoxon is shown in Fig. 5 for two surface concentrations of enzyme, 6.25 and 2.1 U/mL of aliquot (12.5 and 4.2 mU per electrode). Both curves are similar in the range of moderate and high concentrations of an inhibitor. However, the LOD of malaoxon was equal to 0.1 nM for lower enzyme quantity and 7.0 nM for its higher value.

The analytical characteristics of pesticide determination are presented in Table 3. In all the cases the maximal inhibition degrees detected are near 95% indicating fully irreversible character of inhibition. The LOD values were calculated for $S/N=3$.

Performance of the AChE sensor prepared has been compared with some other contemporary biosensors (Table 4). It can be concluded that the AChE sensor developed has higher sensitivity of malaoxon and aldicarb and comparable sensitivity of paraoxon and carbofuran determination. The only sensor with significantly lower LOD is that assembled by polyelectrolyte layers including AChE and carbon nanotubes with multiplication of an inhibition effect exerted by paraoxon due to its accumulation in the surface layer. Meanwhile the AChE sensor based on CB / **TC-0**–Ag composite is easier to prepare and has higher stability and mechanical durability of the surface layer. Also, the incubation period chosen in this work is lower than that commonly used in similar works (10 and 15–20 min, respectively).

For reactivation of AChE after its contact with organophosphate solution the biosensor was treated with 0.1 mM 2-PAM for 10 min followed by careful washing with distilled water and PBS working solution. Additional washing is required because the reactivator itself exerts a weak reversible inhibition of AChE. The reactivation makes it possible to recover up to 90% of initial enzyme activity if the period between inhibition and reactivation does not exceed 30 min. After that, the activity of enzymes decreases. The efficiency of reactivation is higher for inhibition degree lower than 40% and can be used 2–3 times without significant losses in sensitivity of inhibitor determination. It should be mentioned that the use of 2-PAM increases the variation of inhibition at second and third measurement cycles by 30–50%. This limits the number of repetitive uses of the same AChE sensor by 2–3 measurements. The influence of reactivator on inhibition is more pronounced in the middle part of calibration curve corresponding to 20–60% inhibition. The carbamoylated AChE can be reactivated by washing with PBS working solution. The residual inhibition observed in this case was about 15–20% with no respect of the concentration of carbamate and inhibition degree detected. The decay in the sensitivity of inhibition measurement in second and third measurements was less than that observed for phosphorylated AChE but the number of measurements recommended with the same biosensor remains the same (not more than three cycles of inhibition–measurement–reactivation). The decay in the sensitivity observed for reactivated biosensors can be explained by two reasons, i.e. preferable inactivation of the enzyme molecules most accessible for an inhibitor and protecting influence of residual amount of reactivator present in the surface layer after washing.

Although the sensitivity of the pesticide detection is high enough to detect the permissible residuals in fruits and vegetables, it should be mentioned that the use of AChE as a sensing element of biosensor does not allow discrimination of the signal toward different anticholinesterase pesticides. The inhibition of heavy metals is suppressed by the use of PBS at pH=7.8 but in case of a mixture of organophosphates, the resulting inhibition degree can be considered only as an estimate of relative hazard of pollution for a human.

Table 3
The analytical characteristics of pesticide determination, incubation period 10 min.

Pesticide	$\Delta I, \% = a + b \times \log c_I$, M				Concentration range	LOD, nM
	a	b	R^2	n		
Malaoxon	260 ± 17	26 ± 2	0.9942	11	0.4 nM–0.2 μM	0.1
Paraoxon	136 ± 9	11 ± 1	0.9361	14	0.2 nM–0.2 μM	0.05
Carbofuran	131 ± 16	9 ± 1	0.9451	14	0.2 nM–2.0 μM	0.1
Aldicarb	157 ± 5	15 ± 1	0.9615	13	0.01–0.20 μM	10.0

3.6. Reproducibility and stability

The inter-assay precision was characterized by determining the signal of six different AChE sensors to 1.0 mM ATCh solution. The RSD of 2.5% was calculated. The intra-state precision was determined by evaluation of the six repetitive signals of a single AChE sensor toward the same concentration of the substrate. It was found to be 1.1%. Both values indicate acceptable level of repeatability sufficient for inhibition measurement. Each AChE sensor makes it possible to conduct up to 50 measurements of the

Table 4
Comparison of the analytic performance of the AChE sensor developed with recently reported analogous biosensors.

Pesticide	Modifier[a]	LOD (M)	Concentration range (M)	Ref.
Paraoxon	Carbon nanotubes – PDDA self-assembled layers, flow-injection regime	4×10^{-13}	1×10^{-12}–1×10^{-8}	[18]
	Prussian blue/BSA/Nafion	3.6×10^{-8}	5×10^{-8}–1×10^{-6}	[22]
	Carbon nanotubes–TCNQ	3×10^{-11}	1×10^{-10}–5×10^{-8}	[25]
	Polypyrrole/gelatin	4×10^{-9}	4.5×10^{-8}–5.5×10^{-5}	[39]
	Carbon nanotubes Au nanoparticles	1×10^{-9}	1×10^{-10}–7×10^{-9}	[40]
	Carbon nanotubes	5×10^{-10}	5×10^{-10}–7×10^{-9}	[41]
	Au nanoparticles onto cysteamine self-assembled monolayer	7×10^{-9}	7×10^{-9}–1.5×10^{-7}	[42]
	Implementation in the carbon paste	3.6×10^{-9}	4×10^{-9}–1×10^{-5}	[43]
	Polycarboxylated macrocycles, Co phthalocyanine		1×10^{-8}–7×10^{-7}	[44]
	CB/**TC-0**–Ag	5×10^{-11}	2×10^{-10}–2×10^{-7}	This work
Malaoxon	Polycarboxylated macrocycles, Co phthalocyanine	3×10^{-9}	3×10^{-9}–2×10^{-7}	[44]
	Magnetic microbeads on screen-printed electrode	9.4×10^{-9}	1×10^{-8}–1×10^{-6}	[45]
	Sol–gel immobilization in PEI	5×10^{-7}	–	[16]
	CB/**TC-0**–Ag	1×10^{-10}	4×10^{-10}–2×10^{-7}	This work
Aldicarb	Prussian blue/BSA/Nafion	1.5×10^{-7}	2×10^{-7}–2×10^{-6}	[25]
	Au–Pt nanoparticles	4×10^{-5}	4×10^{-5}–4×10^{-4}	[46]
	Co phthalocyanine	1.2×10^{-7}	6×10^{-8}–6×10^{-7}	[47]
	CB/**TC-0**–Ag	1×10^{-8}	1×10^{-8}–2×10^{-7}	This work
Carbofuran	Carbon nanotubes/chitosan/Prussian Blue/nanoAu	2.5×10^{-9}	5×10^{-9}–8×10^{-8}	[24]
	Nafion/BSA/Co phthalocyanine	2.5×10^{-10}	1×10^{-9}–1×10^{-8}	[26]
	Polypyrrole/gelatin	5×10^{-10}	2.2×10^{-8}–2.7×10^{-7}	[39]
	Supported lipid film	1×10^{-9}	1×10^{-9}–1×10^{-7}	[48]
	Fe_3O_4–chitosan	3.6×10^{-9}	5×10^{-9}–9×10^{-8}	[49]
	CB/**TC-0**–Ag	1×10^{-10}	2×10^{-10}–2×10^{-7}	This work

[a] PDDA – poly(diallyldimethylammonium chloride), BSA – bovine serum albumin, TCNQ – tetracyanoquinodimethane.

substrate concentration without any losses of sensitivity. In dry storage conditions at 4 °C, 20% decay of the signal was found after 60 days and 30% after 90 days of storage. However, the repeated drying and cooling the sensor in use significantly decrease the storage stability. At room temperature, the biosensors retained 90% of initial signal during two weeks of operation.

The characteristics of inhibitor detection were estimated in a similar manner with 10 nM malaoxon solution and the RSD values of 7.4% and 9.2% for intra- and inter-assay precision were obtained. During the storage in dry conditions the appropriate characteristics tend to increase to about 15% and 20%, respectively, for 60 days period.

3.7. Application to food samples

The applicability of the AChE sensor is developed for real samples testing, peanut spiked with carbamate pesticides and grape juice spiked with malaoxon and malathion used. All the samples did not contain anticholinesterase pesticides in accordance with HPLC data. Spiked peanut samples were mixed with acetone (1 g per 1 mL) and then vortexed each 2 min within 10 min extraction. After that, an aliquot was taken from the upper layer and mixed with tenfold excess of PBS. No significant influence of acetone present is diluted extract on inhibition degree and sensitivity of pesticide detection was established. Then the inhibition of diluted extract was measured as described above for model aqueous solution of a pesticide. The limit of quantification estimated from $S/N=10$ was found to be 10 nM for carbofuran and 20 nM for aldicarb. This is much lower than tolerance levels established for peanut by Code of Federal Regulations (1 ppm=4.5 μM of carbofuran and 0.05 ppm=0.26 μM of aldicarb [50]). The recovery of the pesticide was calculated from the calibration graph obtained with model solutions. It was equal to 98–105% for 10 nM–1.0 μM carbofuran and 110–130% for 20 nM–1.0 μM aldicarb.

Grape juice as it is exerted reversible inhibition of AChE. For this reason, the juice dilution degree required was found to be higher than that of extract from peanut. First 1 mL of grape juice was mixed with 9 mL of PBS and its pH was adjusted to 7.8. After that, 1 ml of diluted juice was added to the working cell containing 4 mL of PBS working solution and the AChE sensor was incubated in the mixture for 10 min. The recovery was calculated for two concentration of malaoxon, i.e. 10 and 100 nM. In both cases, the recovery was found to be 95–98%. In addition to malaoxon, the same experiments were conducted with its thionic analog, malathion. This pesticide is less toxic for warm-blooded organisms but it is converted to more toxic malaoxon by biochemical oxidation. To increase the sensitivity of malathion detection, the spiked grape juice was first mixed with 0.5% bromine solution in 1:1 v/v ratio as shown below

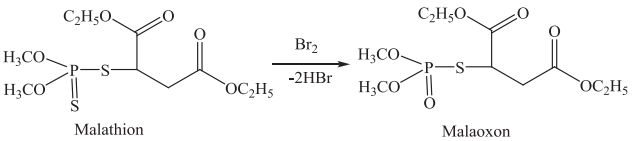

(5)

After 5 min reaction the excess of oxidant was removed by addition of 1 mL of 1.5% formic acid. Then PBS was added to the same final dilution degree as in the case of malaoxon described above. The efficiency of malathion oxidation was near 100%. The inhibition observed for oxidized malathion solution was the same as for malaoxon. The recovery values established for malathion spiked juice samples were equal to 94 ± 5% (10 nM) and 87 ± 7% (100 nM).

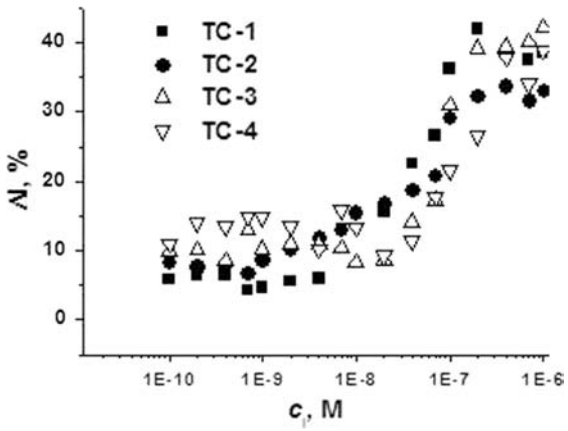

Fig. 6. Calibration plots of malaoxon obtained with AChE sensor based on glassy carbon modified with CB and Ag nanoparticles in the presence of 1.0 μM protecting agents **TC-1**, **TC-2**, **TC-3**, **TC-4**. Incubation 10 min, PBS, pH=7.8.

In addition to spiked samples, the AChE sensors developed were used for testing the potential antidotes able to partially suppress the irreversible inhibition of the enzyme. The protecting effect of reversible inhibition is mainly referred to their competition with irreversible inhibitors for the enzyme active site [51–53]. Contrary to organophosphates, reversible inhibitors are easily leaving the enzyme so that a part of enzyme activity is restored. Regarding AChE, most protecting agents mimic the cationic part of a substrate, i.e., they belong to quaternary ammonia salts or amines. Tetrasubstituted thiacalix[4]arenes exert a weak inhibitory effect on AChE due to formation of non-covalent bonds between cationic terminal groups in the substituents at the lower rim. The length of the linker allows interaction with anionic groups at the enzyme active site followed by decay of the enzyme activity. The maximal inhibition effect is limited by low solubility of the **TC-1**–**TC-4** and is about 20–45% depending on the nature of the substituent. The irreversible inhibition was measured in the mixture of 1.0 μM thiacalix[4]arene **TC-1**–**TC-4** soluble at this level of concentration and varying amounts of malaoxon (Fig. 6). The contribution of malaoxon started from 10 nM, i.e. at the concentration 25 higher than the quantification level of malaoxon at the same conditions (cf., Table 2). Moreover, the upper limit of inhibition was about 50% against 90–100% for all the irreversible inhibitors tested in this work. All the protecting agents tested showed similar shape of the curve which is shifted by 10–15% of inhibition in accordance with relative activity of the protectors in the interaction with AChE. Thus, the thiacalix[4]arenes **TC-1**–**TC-4** exert a remarkable protecting effect which can be used for decreasing the acute toxicity of commercial anticholinesterase pesticides.

4. Conclusion

The application of Ag nanoparticles decorated with a macrocyclic ligand used for their synthesis and involved in the electron transduction together with carbon black as enzyme carrier showed some advantages over common approaches to the modification of amperometric sensors for the AChE biosensor development. The working potential can be decreased to 50 mV though higher accuracy required for inhibition quantification was achieved at 150 mV. The response time was less than 10 s and the lifetime of the AChE sensor kept in dry conditions at 4 °C was equal to three months. In this work, Ag is shielded with macrocycles which prevent direct anodic oxidation of the metal observed for naked particles. The improvement of the sensor

performance in anodic oxidation of thiocholine can result from chemisorption accumulation of thiocholine followed by its mediated oxidation at low overvoltage. The sorptional accumulation of thiocholine was previously described at a non-polarized electrode and at cathodic polarization [54]. The role and relative importance of silver and macrocycles in the improvement of the electrode reactions remain a subject of further investigations. Meanwhile it can be noted that both components are necessary for the final success. Thus the use of CB as enzyme carrier does not lead to such remarkable changes in the measurement conditions.

The AChE sensor developed showed high sensitivity of pesticide determination which is comparable and in some cases exceeds the parameters of other sensors based on mediated electron transfer. This might be due to interactions of insecticides with macrocycles in the proximity of the enzyme due to molecular interactions. Similar reactions have been already described for paraoxon and some other classes of pesticides [55–58]. Being less selective than AChE inhibition, such reactions can decrease the LOD and increase the slope of appropriate calibration curves. The AChE sensor was tested in the detection of residual amounts of pesticides in peanut and grape juice as well as in demonstration of protecting influence of some novel agents with quaternary ammonia groups mimicking the natural substrate structure.

Acknowledgments

The financial support by the Russian Foundation for Basic Research (Grants 12-03-31725 and 12-03-00252-a) is gratefully acknowledged.

Appendix A. Supporting information

Supplementary data associated with this article can be found in the online version at http://dx.doi.org/10.1016/j.talanta.2014.03.048.

References

[1] F. Arduini, A. Amine, D. Moscone, G. Palleschi, Microchim. Acta 170 (2010) 193.
[2] W.N. Aldridge, A.N. Davison, Biochem. J. 55 (1953) 763.
[3] T.R. Fukuto, Environ. Health Perspect. 87 (1990) 245.
[4] D.M. Quinn, Chem. Rev. 87 (1987) 955.
[5] J.S. Van Dyk, B. Pletschke, Chemosphere 82 (2011) 291.
[6] R. Su, X. Xu, X. Wang, D. Li, X. Li, H. Zhang, A. Yu, J. Chromatogr. B 879 (2011) 3423.
[7] C. Hu, M. He, B. Chen, B. Hu, J. Chromatogr. A 1275 (2013) 25.
[8] J.F. Lawrence, C. Renault, R.W. Frei, J. Chromatogr. A 121 (1976) 343.
[9] T.M.G. Valencia, M.P.G. de Llasera, J. Chromatogr. A. 1218 (2011) 6869.
[10] A.C.H. Alves, M.M.P.B. Gonçalves, M.M.S. Bernardo, B.S. Mendes, J. Sep. Sci. 35 (2012) 2653.
[11] G. Fang, W. Chen, Y. Yao, J. Wang, J. Qin, S Wang, J. Sep. Sci. 35 (2012) 534.
[12] M. LeDoux, J. Chromatogr. A 1218 (2011) 1021.
[13] H. Zhang, S. Wang, G. Fang, J. Immunol. Methods 368 (2011) 1.
[14] Z.-L. Xu, Q. Wang, H.-T. Lei, S.A. Eremin, Y.-D. Shen, H. Wang, R.C. Beier, J.-Y. Yang, K.A. Maksimova, Y.-M. Sun, Anal. Chim. Acta 708 (2011) 123–129.
[15] Y.H. Liu, R. Xie, Y.R. Guo, G.N. Zhu, F.B. Tang, J. Environ. Sci. Health B 47 (2012) 475–483.
[16] P. He, J. Davies, G. Greenway, S.J. Haswell, Anal. Chim. Acta 659 (2010) 9.
[17] K. Reybier, S. Zairi, N. Jaffrezic-Renault, B. Fahys, Talanta 56 (2002) 1015.
[18] G. Liu, Y. Lin, Anal. Chem. 78 (2006) 835.
[19] S. Hou, Z. Ou, Q. Chen, B. Wu, Biosens. Bioelectron. 33 (2012) 44.
[20] L.-G Zamfir, L Rotariu, C Bala, Biosens. Bioelectron. 26 (2011) 3692.
[21] F. Arduini, S. Guidone, A. Amine, G. Palleschi, D. Moscone, Sens. Actuators B 179 (2013) 201.
[22] E. Suprun, G. Evtugyn, H. Budnikov, F. Ricci, D. Moscone, G. Palleschi, Anal. Bioanal. Chem. 383 (2005) 597.
[23] S. Wu, X. Lan, W. Zhao, Y. Li, L. Zhang, H. Wang, M. Han, S. Tao, Biosens. Bioelectron. 27 (2011) 82.
[24] C. Zhai, X. Sun, W. Zhao, Z. Gong, X. Wan, Biosens. Bioelectron. 42 (2013) 124.
[25] L. Rotariu, L.-G. Zamfir, C. Bala, Anal. Chim. Acta 748 (2012) 81.
[26] S. Laschi, D. Ogonczyk, I. Palchetti, M. Mascini, Enzym. Microb. Technol. 40 (2007) 485.
[27] G. Valdés-Ramírez, M. Cortina, M.T. Ramírez-Silva, J.-L. Marty, Anal. Bioanal. Chem. 392 (2008) 699.
[28] A.N. Ivanov, R.R. Younusov, G.A. Evtugyn, F. Arduini, D. Moscone, G. Palleschi, Talanta 85 (2011) 216.
[29] D. Liu, W. Chen, J. Wei, X. Li, Z. Wang, X. Jiang, Anal. Chem. 84 (2012) 4185.
[30] N. Dimcheva, E. Horozova, Y. Ivanov, T. Godjevargova, Cent. Eur. J. Chem. 11 (2013) 1740.
[31] C. Parsajoo, J.-M. Kauffmann, Talanta 109 (2013) 116.
[32] W. Tang, J. Wu, Anal. Methods 6 (2014) 924.
[33] G.A. Evtugyn, R.V. Shamagsumova, R.R. Sitdikov, I.I. Stoikov, I.S. Antipin, M. V. Ageeva, T. Hianik, Electroanalysis 23 (2011) 2281.
[34] G. Evtugyn, A. Porfireva, R. Sitdikov, V. Evtugyn, I. Stoikov, I. Antipin, T. Hianik, Electroanalysis 25 (2013) 1847.
[35] E.A. Andreyko, P.L. Padnya, R.R. Daminova, I.I. Stoikov, RSC Adv. 4 (2014) 3556.
[36] B. Bucur, A.F. Danet, J.-L. Marty, Biosens. Bioelectron. 20 (2004) 217.
[37] D.I. Jung, Y.J. Shin, E.S. Lee, T. Moon, C.N. Yoon, B.H. Lee, Bull. Korean Chem. Soc. 24 (2003) 65.
[38] S. Andreescu, L. Barthelmebs, J.-L. Marty, Anal. Chim. Acta 464 (2002) 171.
[39] R.R. Dutta, P. Puzari, Biosens. Bioelectron. 52 (2014) 166.
[40] N. Jha, S. Ramaprabhu, Nanoscale 2 (2010) 806.
[41] K.A. Joshi, J. Tang, R. Haddon, J. Wang, W. Chen, A. Mulchandani, Electroanalysis 17 (2005) 54.
[42] F. Arduini, S. Guidone, A. Amine, G. Palleschi, D. Moscone, Sens. Actuators B 179 (2013) 201.
[43] D. Di Tuoro, M Portaccio, M Lepore, F Arduini, D Moscone, U Bencivenga, D.G Mita, New Biotechnol. 29 (2011) 132.
[44] A.N. Ivanov, R.R. Younusov, G.A. Evtugyn, F. Arduini, D. Moscone, G. Palleschi, Talanta 85 (2011) 216.
[45] N.B. Oujji, I. Bakas, G. Istamboulié, I. Ait-Ichou, E. Ait-Addi, R. Rouillon, T. Noguer, Sensors 12 (2012) 7893.
[46] S. Upadhyay, G.R. Rao, M.K. Sharma, B.K. Bhattacharya, V.K. Rao, R. Vijayaraghavan, Biosens. Bioelectron. 25 (2009) 832.
[47] F. Arduini, F. Ricci, C.S. Tuta, D. Moscone, A. Amine, G. Palleschi, Anal. Chim. Acta 580 (2006) 155.
[48] D.P. Nikolelis, M.G. Simantiraki, C.G. Siontorou, K Toth, Anal. Chim. Acta 537 (2005) 169.
[49] T. Jeyapragasam, R. Saraswathi, Sens. Actuators B 191 (2014) 681.
[50] Code of Federal Regulations. 40. Protection of Environment, 180.254. Carbofuran, 180.269. Aldicarb, Tolerances for Residues, 2006, pp. 360–385.
[51] G.A. Petroianu, M.Y. Hasan, K. Arafat, S.M. Nurulain, A. Schmitt, J. Appl. Toxicol. 25 (2005) 562.
[52] A. Galli, F. Mori, I. Gori, M. Lucherini, Biochem. Pharmacol. 43 (2011) 2427.
[53] S. Eckert, P. Eyer, H. Mückter, F. Worek, Biochem. Pharmacol. 72 (2006) 344.
[54] H. Matsuura, Y. Sato, T Sawaguchi, F Mizutani, Sens. Actuators B 91 (2003) 148.
[55] D. Xiong, H. Li, Nanotechnology 19 (2008) 465502.
[56] C. Li, C. Wang, B. Guan, Y. Zhang, S. Hu, Sens. Actuators B 107 (2004) 411.
[57] Y. Bian, C. Li, H. Li, Talanta 81 (2010) 1028.
[58] G. Bocchinfuso, C. Mazzuca, C. Saracini, M. Venanzi, L. Micheli, G. Palleschi, A. Palleschi, Microchim. Acta 163 (2008) 195.